Experimental Neurology 320 (2019) 113008

Contents lists available at ScienceDirect

Experimental Neurology

journal homepage: www.elsevier.com/locate/yexnr

Research Paper

Activation of GPR30 with G1 attenuates neuronal apoptosis via src/EGFR/stat3 signaling pathway after subarachnoid hemorrhage in male rats

Jun Peng[a,b], Yuchun Zuo[b,c], Lei Huang[b,d], Takeshi Okada[b,e], Shengpeng Liu[a,b], Gang Zuo[b,f], Guangyu Zhang[b], Jiping Tang[b], Ying Xia[a,**], John H. Zhang[b,d,g,*]

[a] Department of Neurosurgery, Central South University Xiangya School of Medicine Affiliated Haikou Hospital, Haikou, Hainan 570000, China
[b] Department of Physiology and Pharmacology, Loma Linda University, Loma Linda, CA 92354, USA
[c] Department of Neurosurgery, The Third Xiangya Hospital, Central South University, Changsha, Hunan 410013, China
[d] Department of Neurosurgery, Loma Linda University, Loma Linda, CA 92354, USA
[e] Department of Neurosurgery, Mie University, Tsu, Mie 514-8507, Japan
[f] Department of Neurosurgery, Taicang People's Hospital, Taicang 215400, Jiangsu, China
[g] Department of Anesthesiology, Loma Linda University, Loma Linda, CA 92354, USA

ARTICLE INFO

Keywords:
GPR30
GPER1
Estrogen receptor
G1
Subarachnoid hemorrhage
Early brain injury
Apoptosis
Bcl-2
Rat

ABSTRACT

Background: Neuron apoptosis plays a vital role in early brain injury (EBI) after subarachnoid hemorrhage (SAH). Previous studies showed that the activation of G protein-coupled receptor 30 (GPR30) with GPR30 agonist G1 was anti-apoptotic after experimental trauma brain injury and global cerebral ischemia in male rats or mice. However, the role of GPR30 activation with G1 has not been clarified in SAH. The aim of this study was to investigate the anti-apoptotic effect of GPR30 activation and the underlying mechanism of src/EGFR/stat3 signaling pathway in a male rat model of SAH.

Methods: A total of 215 male rats and 18 female rats were used. SAH was induced by intravascular perforation. G1 was administrated intravenously 1 h after SAH. For mechanism study, the GPR30 antagonist G15 or epidermal growth factor receptor (EGFR) antagonist AG1478 was administrated intravenously 1 h before SAH, small interfering ribonucleic acid (siRNA) for GPR30 and EGFR were administered intracerebroventricularly 48 h before SAH. Post-SAH assessments included SAH Grade, neurological deficits, western blot, terminal deoxynucleotidyl transferase dUTP-biotin nick end labeling (TUNEL) staining, Fluoro-Jade C (FJC) staining, Nissl staining and immunofluorescence.

Results: The expression of endogenous GPR30 in male rats was increased at 3 h and peaked at 24 h after SAH, which mainly co-localized with neurons, but there was no significant increase in intact female rats at 24 h after SAH. The G1 post-treatment significantly reduced the short-term and long-term neurological deficit as well as neuronal apoptosis in male rats, but it did not significantly improve the short-term outcome of intact female rats. Mechanistic studies indicated that G15 or GPR30 siRNA and AG1478 or EGFR siRNA reversed the anti-neuronal apoptosis effects of G1 and its effects on protein expressions of src/EGFR/stat3 signaling pathway.

Conclusion: G1 reduced EBI through attenuating neuronal apoptosis after SAH in male rats, partly via activating src/EGFR/stat3/signaling pathway. G1 may provide a promising therapeutic strategy for SAH patients.

1. Introduction

Subarachnoid hemorrhage (SAH) is a type of hemorrhagic stroke with high mortality and disability (>50%) (Fujii et al., 2013). Emerging evidence has shown that early brain injury (EBI) plays an important pathological role in SAH (Wei et al., 2017). EBI emphasizes the immediate global brain injury caused by the temporary increased intracranial pressure and reduced cerebral blood flow after the rupture of aneurysm (Conzen et al., 2018). One of the main pathophysiological mechanisms contributing to the EBI development is activation of

* Correspondence to: J. H. Zhang, Department of Physiology and Pharmacology, Loma Linda University, 11234 Anderson St, Room 2562B, Loma Linda, CA 92354, USA.
** Correspondence to: Y. Xia, Department of Neurosurgery, Central South University Xiangya School of Medicine Affiliated Haikou Hospital, Haikou, Hainan 570000, China.
E-mail addresses: xiaying008@163.com (Y. Xia), johnzhang3910@yahoo.com (J.H. Zhang).

https://doi.org/10.1016/j.expneurol.2019.113008
Received 1 March 2019; Received in revised form 16 May 2019; Accepted 5 July 2019
Available online 08 July 2019
0014-4886/

apoptotic pathway and the anti-apoptosis treatments were effective therapeutic strategies against EBI (Cahill et al., 2007; Shi et al., 2017; Yan et al., 2017; Zhao et al., 2018).

G protein-coupled receptor 30 (GPR30), also known as G protein-coupled estrogen receptor 1 (GPER1), has been considered as a novel membrane estrogen receptor (mER) that mediates the rapid non-genomic actions of estrogen by stimulating the intracellular second messenger signals (Thomas et al., 2005). GPR30 mainly mediates the neuroprotective (Tang et al., 2014; Zhao et al., 2016a), anorexia (Kwon et al., 2014) and anxiogenic (Kastenberger et al., 2012) effects of estrogen in central nervous system (CNS). It was also found to mediate the acute vascular effects of aldosterone in aortic smooth muscle cells (Gros et al., 2011). G1, the agonist of GPR30, selectively activates GPR30 without binding to other nuclear ERs such as ERa or ERβ (Burai et al., 2010). Although G1 activated ERa-36 in SKBR3 cells (Kang et al., 2010), the blocking of GPR30 with G15 (GPR30 antagonist) abolished the neuroprotective effect of G1 (Dennis et al., 2009). It suggested that ERa-36 did not mediate the protective effects of G1. Previous studies showed that activation of GPR30 with G1 could mimic the anti-apoptotic effects of estrogen in animal model of traumatic brain injury (TBI) (Day et al., 2013) and global cerebral ischemia (GCI) (Kosaka et al., 2012) in male rats or mice. However, the role of GPR30 activation has not been elucidated in the setting of SAH.

In breast cells, the activation of GPR30 trans-activated epidermal growth factor receptor (EGFR) via src signaling to promote the cell survival (Filardo, 2002; Filardo et al., 2002). Upon the activation of EGFR, signal transducers and activators of transcription 3 (stat3) was phosphorylated (Park et al., 1996). The phosphorylated stat3 (p-stat3) dimerized and translocated into the nuclear to up-regulate the transcription of anti-apoptosis gene Bcl-2 (Fukada et al., 1996). Previous studies have reported that GPR30 exerted its neuroprotective effect through PI3K/Akt or MAPK/ERK signaling pathway (Cheng et al., 2016; Liu et al., 2011), but it is not clear whether src/EGFR/stat3 signaling also contributes to the anti-apoptotic effect of G1 after brain injury.

Taken together, we proposed the hypothesis that the activation of GPR30 with G1 would reduce EBI through attenuating neuronal apoptosis in male rats after SAH. Such anti-apoptotic effects would be partly via src/EGFR/stat3 signaling pathway.

2. Materials and methods

2.1. Animals

Two hundred and fifteen adult male Sprague-Dawley (SD) rats and eighteen adult female Sprague-Dawley (SD) rats (Indianapolis, IN, weighing 280 to 320 g) were used according to the experimental protocol approved by the Institutional Animal Care and Use Committee of Loma Linda University. The guidelines of ARRIVE and NIH was followed strictly during the animal use. All of the rats were housed in a room which was suitable for temperature and humidity. The rats were raised with unlimited water and food. All of the rats went through a 12 h cycle of day and night.

2.2. SAH model

The endovascular perforation model of SAH was induced as previously reported (Guo et al., 2016). Briefly, anesthetized with 3% isoflurane, the rats were intubated and ventilated. The carotid artery and its branches were separated in the left carotid triangle. The sharpened, 4–0 monofilament nylon was sutured into the vascular cavity when the left external carotid artery was cut off. The nylon was further sutured into the left brain follow the left internal carotid artery, until the bifurcation of the anterior and middle cerebral arteries was punctured. The suture was withdrew quickly. The hemostasis at the puncture site was reached by electrocoagulation, followed by the ligation of the broken end of external carotid artery. Rats in sham groups went through the same surgical process without puncture. When the autonomous respiration returned, the rats were discontinued from ventilation and allowed to recover in a heated blanket.

2.3. Drug administration

G1 (agonist of GPR30, CAS NO 881639-98-1, Cayman Chemical, MI, USA), G15 (antagonist of GPR30, CAS NO. 1161002-05-6, Cayman Chemical, MI, USA), AG1478 (antagonist of EGFR, ab141438, Abcam, Cambridge, MA, USA) were all dissolved in 10% DMSO and administrated intravenously (i.v.) through femoral vein. GPR30 siRNA (sc-156143, Santa Cruz Biotechnology, Inc., TX, USA), EGFR siRNA (sc-108050, Santa Cruz Biotechnology, Inc., TX, USA) were administrated intracerebroventricularly (i.c.v.). Equal volumes of 10% DMSO and Control siRNA-A (sc-37007, Santa Cruz Biotechnology, Inc., TX, USA) were administrated i.v. or i.c.v. to the rats as the vehicle. The intracerebroventricular injection was performed as previously described (Akyol et al., 2018). Rats were placed in a stereotaxic apparatus under 2.5% isoflurane anesthesia. The needle of a 10 μL Hamilton syringe (Microliter 701, Hamilton Company, USA) was inserted through a burr hole into the left ventricle at the following coordinates relative to bregma: 1.5 mm lateral, 0.9 mm posterior, and 3.3 mm beneath the horizontal plane of the skull. GPR30 siRNA, EGFR siRNA and Control siRNA were infused into ventricle at a rate of 1 μL/min (100 pm/μL, 5 μL) by a pump, and the needle was kept in place for 5 min after the end of each injection to prevent reflux.

2.4. Experimental design

Experiment 1: Time course and cellular localization of GPR30 in male rats

In this part, forty adult male SD rats were randomly divided into the following six groups: Sham and SAH (3 h, 6 h, 12 h, 24 h, 72 h). The endogenous expression of GPR30 were detected by western blot in each group ($n = 6$). The double immunofluorescence labeling of GPR30 with neuronal nuclei (NeuN), glial fibrillary acidic protein (GFAP) and calcium-binding adaptor molecule1(Iba-1) were performed in sham group and SAH (24 h) group ($n = 2$).

Experiment 2: The effect of G1 on short-term outcome study in male and intact female rats

In this part, thirty male rats were randomly and equally divided into the following five groups with n = 6/group: Sham; SAH + Vehicle; SAH + G1(100μg/kg); SAH + G1(300μg/kg); SAH + G1(900μg/kg). Eighteen intact female rats were randomly and equally divided into the following three groups with n = 6/group: Sham; SAH + Vehicle; SAH + G1(300μg/kg). The neurological deficit was evaluated by Modified Garcia scale and Beam Balance test at 24 h after SAH. The neuronal apoptosis and degeneration in male rats were evaluated by terminal deoxynucleotidyl transferase dUTP-biotin nick end labeling (TUNEL) staining and Fluoro–Jade C staining. The protein level of GPR30 and Bcl-2 in intact female rats were detected by western blot. G1 or vehicle was administrated i.v. at 1 h after SAH. The mortality and SAH Grade were recorded during the process.

Experiment 3: The effect of G1 on long-term outcome study of male rats

In this part, thirty male rats were randomly and equally divided into the following three groups with $n = 10$/group: Sham; SAH + Vehicle; SAH + G1. G1 (best dose) was administrated i.v. at 1 h after SAH, The sensorimotor coordination and balance ability was evaluated by Rotarod test at day 7, day 14 and day 21 after SAH. The spatial learning

A

Groups	Mortality	Excluded
Experiment 1: Time course and cellular localization		
Sham (n=8)	0.00%(0/8)	0
SAH(3h,6h,12h,24h,72h) (n=32)	18.60%(8/43)	3
Experiment 2: Short-term outcome study		
Sham (n=16)	0.00%(0/16)	0
SAH+Vehicle (n=16)	15.00%(3/20)	1
SAH+G1(100μg/kg) (n=6)	12.50%(1/8)	1
SAH+G1(300μg/kg) (n=16)	10.53%(2/19)	1
SAH+G1(900μg/kg) (n=6)	11.11%(1/9)	2
Experiment 3: Long-term outcome study		
Sham (n=10)	0.00%(0/10)	0
SAH+Vehicle (n=10)	16.67%(2/12)	0
SAH+G1(300μg/kg) (n=10)	16.67%(2/12)	0
Experiment 4: Mechanism		
Sham (n=6)	0.00%(0/6)	0
SAH+Vehicle (n=6)	22.22%(2/9)	1
SAH+G1 (n=6)	12.50%(1/8)	1
SAH+G15 (n=6)	14.29%(1/7)	0
SAH+AG1478 (n=6)	14.29%(1/7)	0
SAH+G1+DMSO (n=6)	0.00%(0/6)	0
SAH+G1+G15 (n=6)	0.00%(0/7)	1
SAH+G1+GPR30 siRNA (n=6)	14.29%(1/7)	0
SAH+G1+AG1478 (n=6)	0.00%(0/6)	0
SAH+G1+EGFR siRNA (n=6)	14.29%(1/7)	0
SAH+G1+Control siRNA (n=6)	0.00%(0/6)	0
Total		
Sham	0.00%(0/46)	0
SAH	13.90%(26/187)	11

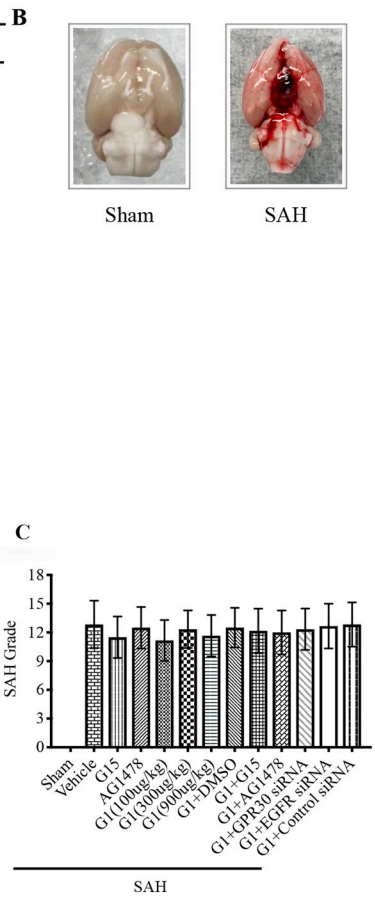

Fig. 1. Mortality and SAH grade. (A) The numbers of the rats used and excluded as well as the mortality in each group. (B) The representative pictures of brains in Sham and SAH group showed that the blood clots were mainly distributed around the Circle of Willis after SAH. (C) SAH Grade in each group. There was no significant difference of grade score among all SAH groups.

and reference memory functions were evaluated by Morris Water Maze test at day 21–25 after SAH. The neuronal loss of hippocampus CA1 was evaluated by Nissl staining at day 25 after SAH. The mortality and SAH Grade were also recorded during the process.

Experiment 4: Mechanism study

In this part, sixty-six male rats were randomly and equally divided into the following eleven groups with $n = 6$/group: Sham; SAH + Vehicle; SAH + G1; SAH + G15; SAH + AG1478; SAH + G1 + DMSO; SAH + G1 + G15; SAH + G1 + AG1478; SAH + G1 + Control siRNA; SAH + G1 + GPR30 siRNA; SAH + G1 + EGFR siRNA. G15 (1 mg/kg) and AG1478 (1 mg/kg) were administrated i.v. at 1 h before SAH. GPR30 siRNA and EGFR siRNA were administrated i.c.v. at 48 h before SAH. G1 (best dose) was administrated i.v. at 1 h after SAH. The neurological deficit was evaluated by Modified Garcia scale and Beam Balance test at 24 h after SAH. In addition, the protein level of p-src/src; p-EGFR/EGFR; p-stat3/stat3; Bcl-2 and cleaved caspase-3 in ipsilateral hemisphere were detected by western blot. The mortality and SAH Grade were also recorded during the process.

2.5. SAH grade

SAH Grade was used to evaluate the severity of SAH as previously published (Sugawara et al., 2008). The basal cistern was divided into six sections, each section was given a grade of 0–3 as follows: 0 = no SAH; 1 = minimal SAH; 2 = SAH with recognizable vessels; 3 = SAH without recognizable vessels. The total score ranging from 0 to 18, the rats with the score < 8 were excluded.

2.6. Modified Garcia scale and Beam balance test

At 24 h after SAH, Modified Garcia scale and Beam balance test were performed to evaluate the neurological deficit as previously described (Zhou et al., 2018). Modified Garcia scale consists of spontaneous activity in cage for 5 min (score from 0 to 3); spontaneous movements of all limbs (score from 0 to 3); movement of forelimbs (score from 0 to 3); climbing wall of wire cage (score from 1 to 3); touch of trunk (score from 1 to 3); vibrissae touch (score from 1 to 3), the total score ranging from 3 to 18. Beam Balance test is to place the rats on the beam and then observe the walking distance within 1 min: 0 = not walk and fall; 1 = not walk, but remains on beam; 2 = walk but fall; 3 = walk $<$ 20 cm; 4 = walk beyond 20 cm, take the average after three repetitions.

2.7. Rotarod test and Water Maze test

At day 7, day 14 and day 21 after SAH, Rotarod test was performed to evaluate the sensorimotor coordination of rats as previously reported (Xie et al., 2018). The rotarod speed started from 5 rpm (RPM) and 10 RPM, the speed increased 2 RPM per 5 s. The duration of rats staying on the accelerating rotating cylinder was recorded. Morris Water Maze test was performed at day 21–25 to evaluate the long term spatial learning and reference memory functions of rats as previously reported (Bromley-Brits et al., 2011). At day 25, the rats were tested with a 60s probe trial to find the platform which had been removed from the water. The action trail of rats including the escape latency, path length

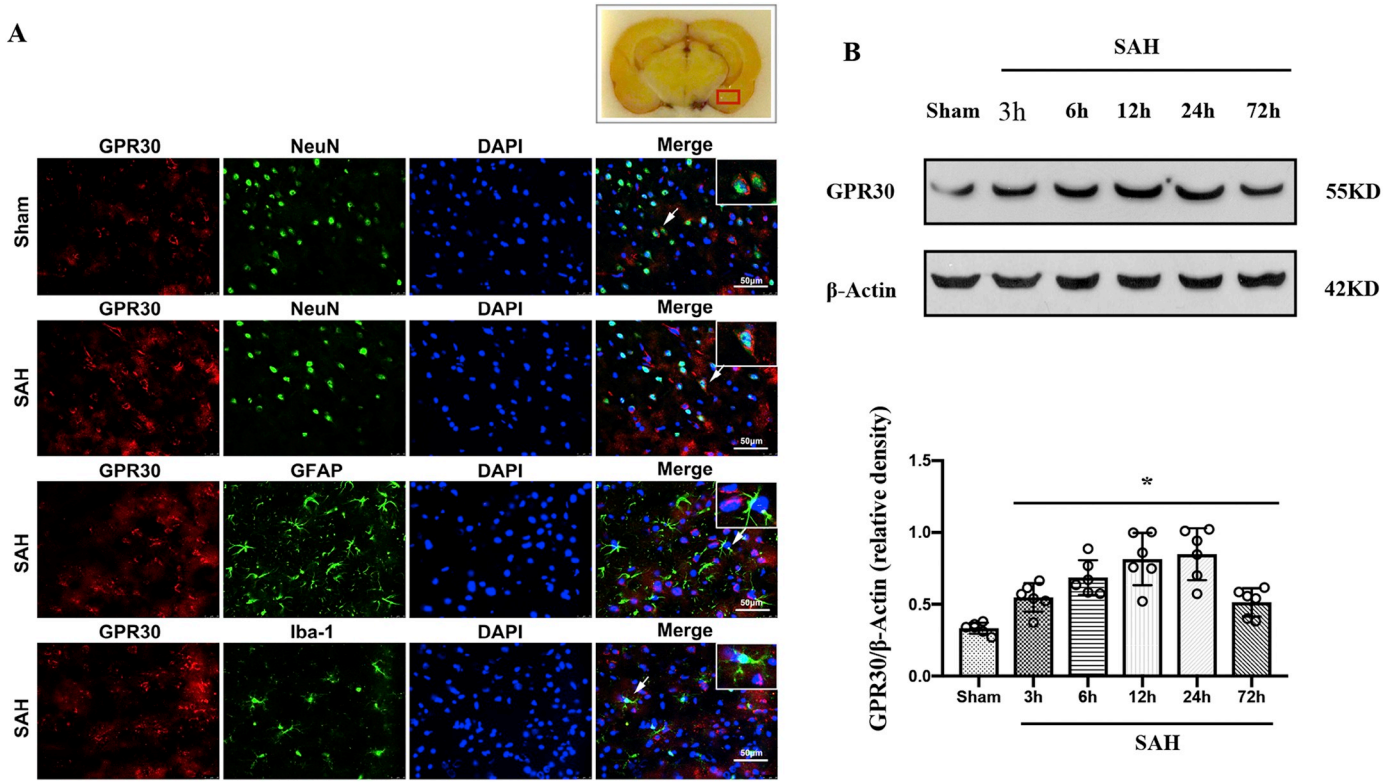

Fig. 2. The endogenous expression of GPR30 in ipsilateral hemisphere was increased at 24 h after SAH in male rats and it was mainly located in neurons. (A) The representative microphotographs of double immunofluorescence labeling showed that GPR30 (red) co-localized with NeuN-positive neurons (green) in both Sham and SAH groups ($n = 2$ for each group). The red rectangle in coronal brain section indicated the brain location of staining. (B) The representative western blot image and quantitative analysis of GPR30 in the ipsilateral hemisphere showed GPR30 expression was increased at 3 h, peaked at 24 h and started declining at 72 h after SAH. Data were presented as mean ± SD ($n = 6$ for each group). $^{*}P < .05$ vs. Sham group. (For interpretation of the references to colour in this figure legend, the reader is referred to the web version of this article.)

and probe quadrant duration as well as swimming velocity were recorded and analyzed by the video tracking system SMART-2000 (San Diego Instruments Inc., CA, USA).

2.8. Double immunofluorescence labeling

At 24 h after SAH, the rats were deeply anesthetized and perfused with ice pre-cold 0.1 M PBS and followed by 10% formalin. The extracted rats brains were fixed in 10% formalin for 48 h at 4 °C and dehydrated in 30% sucrose solution until it sank to the bottom. The coronal frozen sections (10 μm) were sliced and mounted on the slide glass. Brain slices were rinsed 3 times for 5 min/time with 0.1 M PBS. The cell membranes were destroyed with 0.3% triton x-100 for 1 h and the brain slice was blocked with 5% donkey serum for 2 h at room temperature. The brain slices were incubated with the following primary antibodies: rabbit anti-GPR30 (1:100, ab3974, Abcam, MA, USA); mouse anti-NeuN (1:100, ab177487, Abcam, MA, USA); mouse anti-Iba1 (1:100, ab15690, Abcam, MA, USA); mouse anti-GFAP (1:100, ab7260, Abcam, MA, USA) at 4 °C overnight. After washed 3 times for 5 min/time with 0.1 M PBS, the brain slices were incubated with the fluorescence dye-conjugated secondary antibodies (1:200, Jackson ImmunoResearch, PA, USA) on condition of avoiding light for 2 h at room temperature. The brain slices were washed 3 times for 5 min/time with 0.1 M PBS and then covered by cover slips after adding the DAPI. The cellular localization of the GPR30 was observed and photographed under the fluorescence microscope (Olympus, Melville, NY, USA).

2.9. TUNEL staining

Double staining of TUNEL and NeuN was performed to evaluate the neuronal apoptosis at 24 h after SAH. After incubating the primary antibody:mouse anti-NeuN (1:100, ab177487, Abcam, MA, USA), the fluorescence dye-conjugated secondary antibodies (1:200, Jackson ImmunoResearch, PA, USA) was added into the apoptosis detect kit (12156792910, Roche, MO, USA) and then co-incubated for 2 h. The other process was the same as that of double immunofluorescence labeling. Six brain slices per brain were observed under the fluorescence microscope with high magnification (400×). TUNEL positive cells were quantitatively analyzed by ImageJ software (ImageJ 1.5, NIH, USA). Data were presented as TUNEL-positive cells/field.

2.10. Fluoro-Jade C staining

Fluoro-Jade C (FJC) staining was performed to evaluate the neuron degeneration at 24 h after SAH. Fluoro-Jade C Ready-to-Dilute Staining Kit (Biosensis, USA) were used according to the manufacture instruction. Six brain slices per brain were observed under the fluorescence microscope with high magnification (400×). FJC positive cells were quantitatively analyzed by ImageJ software (ImageJ 1.5, NIH, USA). Data were presented as FJC-positive cells/field.

2.11. Nissl staining

Nissl staining was performed to evaluate the neuronal loss of hippocampus CA1 at day 25 after SAH. After rewarming and drying the coronal section, the tissue was dehydrated in 95% and 70% ethanol successively for 1 min, then the section were rinsed in distilled water for 30 s and stained in 1% cresyl velet for 3 min. The section were dehydrated in 100% ethanol for 90 s after it was washed in distilled water for 30 s. Before coverslips were applied with neutral balsam, the slides

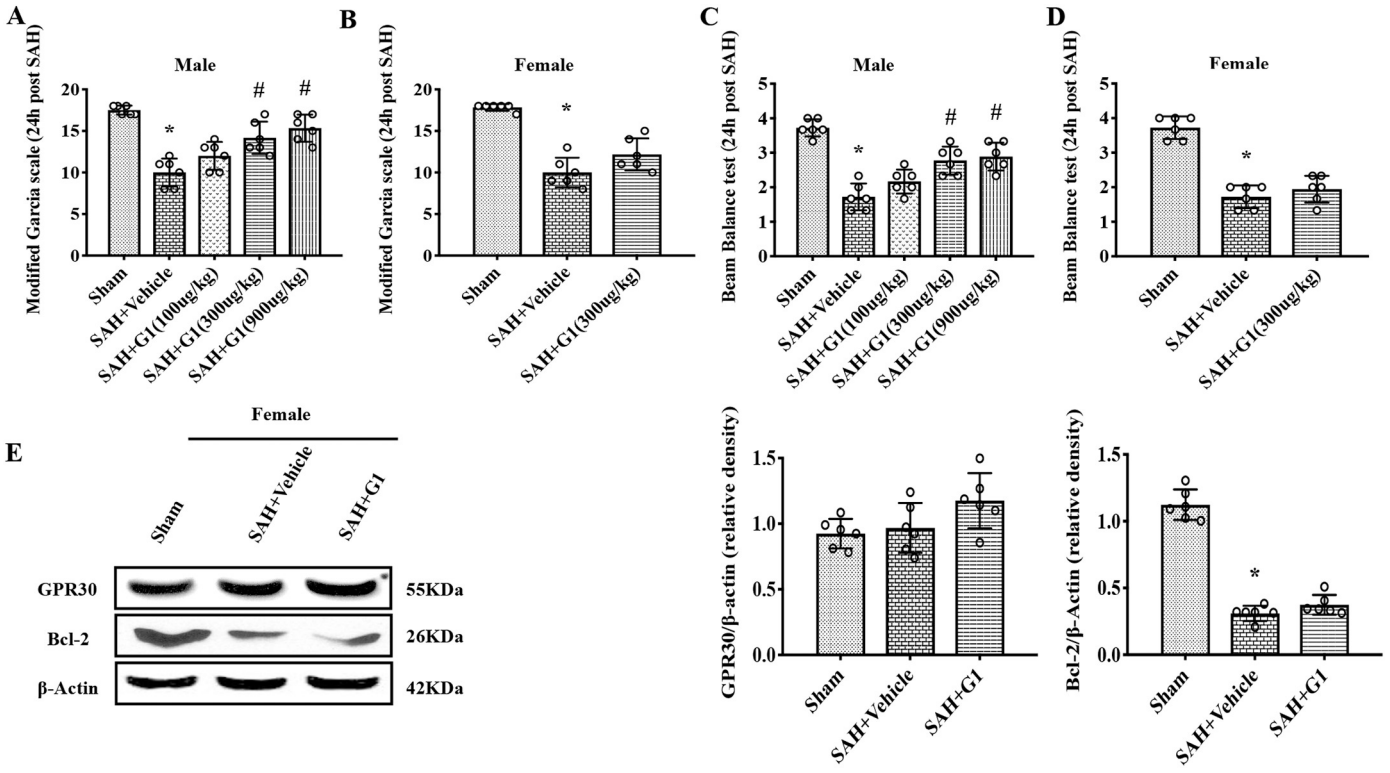

Fig. 3. The G1 post-treatment reduced short-term neurological deficits of male rats but not female rats and it did not promote the expression or activity of GPR30 to prevent down-regulation of Bcl-2 at 24 h after SAH. The endogenous expression of GPR30 in ipsilateral hemisphere was not increased at 24 h after SAH in intact female rats. The neurological functions evaluated by Modified Garcia scale (A,B) and Beam Balance test (C,D) showed that G1 post-treatment significantly reduced the neurological deficits of male rats but not intact female rats at 24 h after SAH (n = 6 for each group). The protein level of GPR30 in ipsilateral hemisphere of intact female rats detected by western blot (E) showed that SAH did not promote the expression of GPR30 and G1 post-treatment did not improve the expression or activity of GPR30 to prevent down-regulation of Bcl-2 at 24 h after SAH. Data were presented as mean ± SD (n = 6 for each group). $^{*}P < .05$ vs. Sham group, $^{\#}P < .05$ vs. SAH + Vehicle group.

were given two 2 min passes in 100% xylene. The numbers of surviving neurons/field(400×) in hippocampal CA1 were counted.

2.12. Western blot

Western blot was performed as previously described (Pang et al., 2018). At 3 h, 6 h, 12 h, 24 h, 72 h, after SAH, the rats were deeply anesthetized and perfused with ice pre-cold 0.1 M PBS. After PBS perfusion, the left (ipsilateral) hemisphere was extracted and mixed with the cell lysate (sc-24,948, Santa Cruz Biotechnology Inc., TX, USA; 300 mg tissue/1 mL cell lysate). The brain tissue were homogenized and centrifuged at 15000gX20min, 4 °C and the supernatant was collected. After the determination of protein concentration, equal protein sample was separated by different concentration of SDS-PAGE gel (7.5%, 10% and 12%), then transferred onto nitrocellulose membranes. The membrane were blocked with 5% non-fat milk for 2 h at room temperature and incubated with the following primary antibodies overnight at 4 °C: Anti-GPR30 (1:1000, ab39742, Abcam, Cambridge, MA, USA); Anti-src (phosphoY419) (1:500, ab185617, Abcam, Cambridge, MA, USA); Anti-src (1:1000, ab47405, Abcam, Cambridge, MA, USA); Anti-EGFR (phosphoY1068) (1:1000, ab40815, Abcam, Cambridge, MA, USA); Anti-EGFR (1:1000, ab52894, Abcam, Cambridge, MA, USA); Anti-stat3 (1:1000, ab119352, Abcam, Cambridge, MA, USA); Anti-stat3 [phosphoY705] (1:500, ab76315, Abcam, Cambridge, MA, USA); Anti-Bcl-2 (1:1000, ab59348, Abcam, Cambridge, MA, USA); Cleaved Caspase-3 (1:500, #9661, Cell Signaling Technology, MA, USA); Anti-β-actin (1:1000, sc- 47,778, Santa Cruz Biotechnology Inc., TX, USA). On the following day, the membrane were washed and then incubated with corresponding secondary antibodies (1:3000, Santa Cruz Biotechnology Inc., TX, USA) for 2 h at room temperature. The bands were visualized with the ECL Plus chemiluminescence reagent kit (Amersham Bioscience, Arlington Heights, IL, USA). Analysis of the densitometry was performed with Image J and the results were reported as a relative density ratio.

2.13. Statistical analysis

All statistical analyses were performed by Graph Pad Prism 6.0 for MAC (La Jolla, CA, USA). The data were expressed as mean ± SD. The comparisons between groups were analyzed by one-way analysis of variance (ANOVA), followed by Tukey multiple comparisons test. $P < .05$ was considered as statistically significant.

3. Results

3.1. Mortality and SAH grade

A total number of 215 male rats and 18 female rats were used in this study, in which 11 rats were excluded due to mild SAH. As shown in Fig. 1A, the total mortality of SAH rats were 13.90% (26/187) and none of sham animals died (0/46). In SAH rats, the blood clots were mainly distributed around the Circle of Willis (Fig. 1B). The SAH Grade score ranging from 9 to 16 in SAH group which were not significant different among the experimental SAH groups (Fig. 1C).

3.2. The expression of GPR30 was mainly located in neurons in male rats and was increased in ipsilateral hemisphere in male rats but not intact female rats after SAH

Double immunofluorescence labeling and western blot were

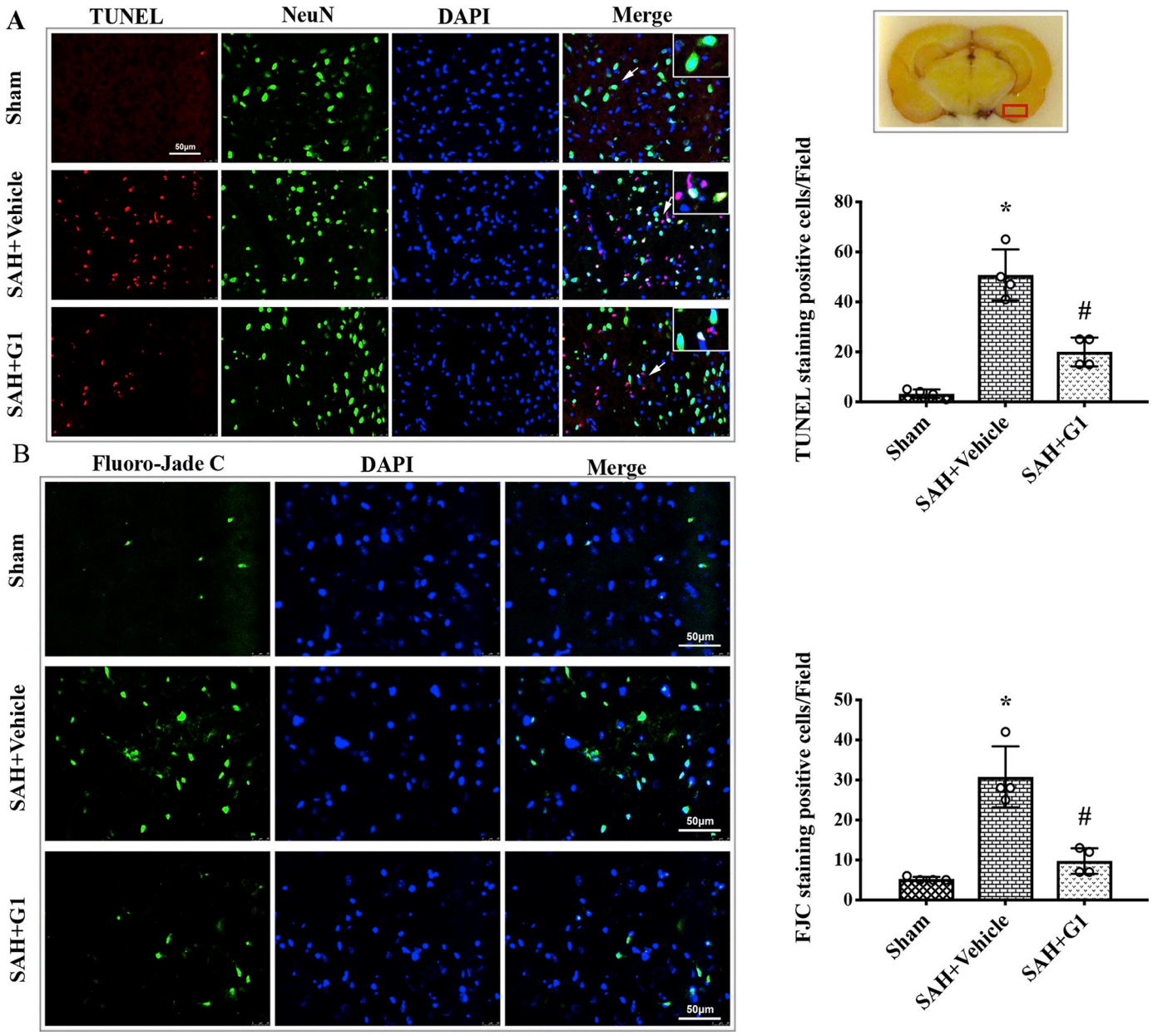

Fig. 4. The G1 post-treatment attenuated neuronal apoptosis of male rats at 24 h after SAH. The representative microphotographs and quantitative analysis for TUNEL staining (A) and Fluoro-Jade C staining (B) in ipsilateral hemisphere cortex consistently demonstrated that there were significantly less neuronal apoptosis and degeneration in G1 treated male SAH rats at 24 h after SAH ($n = 4$ for each group). Data were presented as mean ± SD. $^{*}P < .05$ vs. Sham group, $^{\#}P < .05$ vs. SAH + Vehicle group.

performed to detect the cellular localization and the endogenous protein level of GPR30 in ipsilateral hemisphere after SAH respectively. The results showed that the GPR30 colocalized with NeuN positive neurons but not GFAP/Iba-1 positive astrocytes/microglia cells at 24 h after SAH in male rats (Fig. 2A). The expression of GPR30 in male rats was increased significantly at 3 h, peaked at 24 h and started declining at 72 h after SAH (Fig. 2B). But in intact female rats, the expression of GPR30 in ipsilateral hemisphere was not increased significantly at 24 h after SAH (Fig. 3E). It indicated that SAH promoted the endogenous expression of GPR30 in the ipsilateral hemisphere in male rats but not intact female rats at 24 h and it was mainly expressed by neurons in male rats.

3.3. G1 reduced the neurological deficit in male rats but not intact female rats at 24 h after SAH, which was associated with attenuated neuronal apoptosis and degeneration

Modified Garcia scale (Fig. 3A,B) and Beam Balance test (Fig. 3C,D) were performed to evaluate the neurological deficit at 24 h after SAH. The results showed that G1 at the dose of 300 μg/kg and 900 μg/kg, but not 100 μg/kg significantly reduced the neurological deficit of male rats compared with SAH + Vehicle group. But G1(300μg/kg) did not significantly reduce the neurological deficit and prevent down-regulation of Bcl-2 in intact female rats compared with SAH + Vehicle group (Fig. 3E). Based on the neurological function results, the 300 μg/kg was used as the best dose of G1 in male rats for TUNEL staining, FJC staining, the long-term neurological function study and mechanistic study.

TUNEL staining (Fig. 4A) and FJC staining (Fig. 4B) were performed

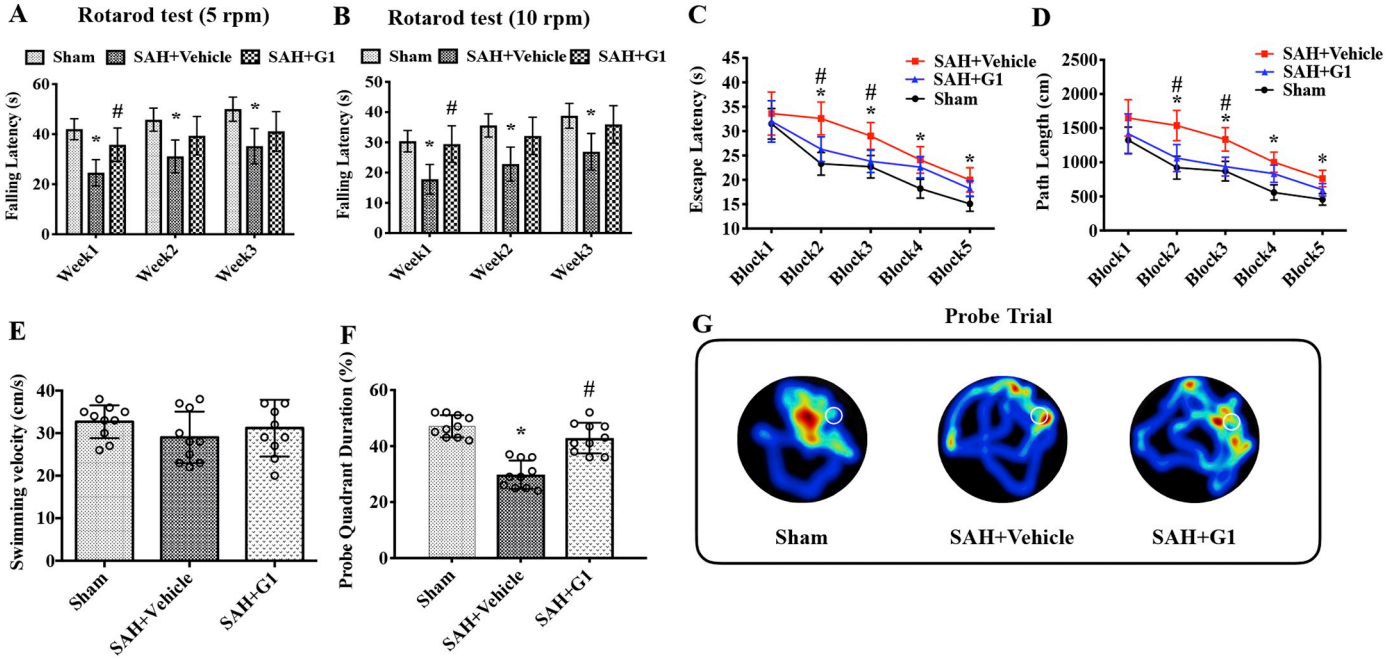

Fig. 5. The G1 post-treatment improved the long-term neurobehavior of male rats after SAH. G1 treatment significantly improved the performance of Rotarod test at 5 rpm (A) and Rotarod test at 10 rpm (B) at week 1 after SAH. Water Maze test showed that G1 treated SAH rats needed significantly less time (C) and swimming distance (D) to find the probe at Block 2 and Block 3. In probe quadrant trial, swimming velocities (E) among groups were not significantly different. Quantification of the probe quadrant duration (F) and representative heat-maps (G) showed that G1 treated SAH rats spent more time within the probe quadrant. Data were presented as mean ± SD (n = 10 for each group). $^{*}P < .05$ vs. Sham group, $^{\#}P < .05$ vs. SAH+ Vehicle group.

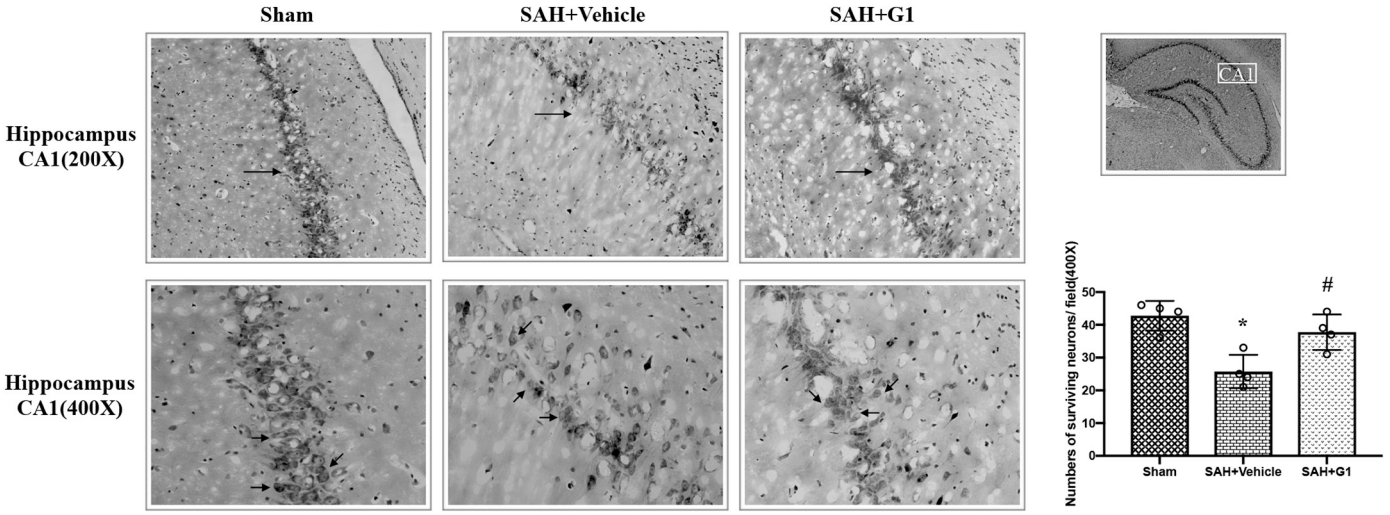

Fig. 6. The G1 post-treatment attenuated the neuronal loss of hippocampus CA1 at day 25 after SAH in male rats. Nissl staining were performed to evaluate the neuronal loss of hippocampus CA1 at day 25 after SAH in male rats. The results showed that SAH increased the neuronal loss of hippocampus CA1 but G1 post-treatment attenuated the neuronal loss. Data were presented as mean ± SD (n = 10 for each group). $^{*}P < .05$ vs. Sham group, $^{\#}P < .05$ vs. SAH+ Vehicle group.

to evaluate the neuronal apoptosis and degeneration at 24 h after SAH. The results showed that both TUNEL and FJC positive neurons in SAH + Vehicle group were significantly increased compared with sham group. However, G1 treatment significantly reduced TUNEL and FJC positive neurons after SAH. The results indicated that G1 significantly attenuated the neuronal apoptosis and degeneration at 24 h after SAH in male rats.

3.4. G1 improved long-term sensorimotor coordination and spatial learning as well as reference memory functions, reduced the neuronal loss of hippocampus CA1 after SAH in male rats

Rotarod test was performed to evaluate the sensorimotor coordination function of rats at week 1, week 2 and week 3 after SAH. Rotarod test at both 5 rpm (Fig. 5A) and 10 rpm (Fig. 5B) showed that SAH significantly decreased the falling latency compared with Sham group at week 1, week 2 and week 3, but G1 treatment significantly improved the performance of Rotarod test at week 1 compared with SAH + Vehicle group. It indicated that G1 increased the sensorimotor coordination function of male rats at week 1 after SAH.

Morris Water Maze test (Fig. 5 C-G) was performed to evaluate the long-term spatial learning and reference memory functions of rats at day 25 after SAH. The results showed that more escape latency (Fig. 5C), longer path length (Fig. 5D) and less time in probe quadrant (Fig. 5F) were observed in SAH + Vehicle group than sham group; However, less escape latency and shorter path length at block 2 and

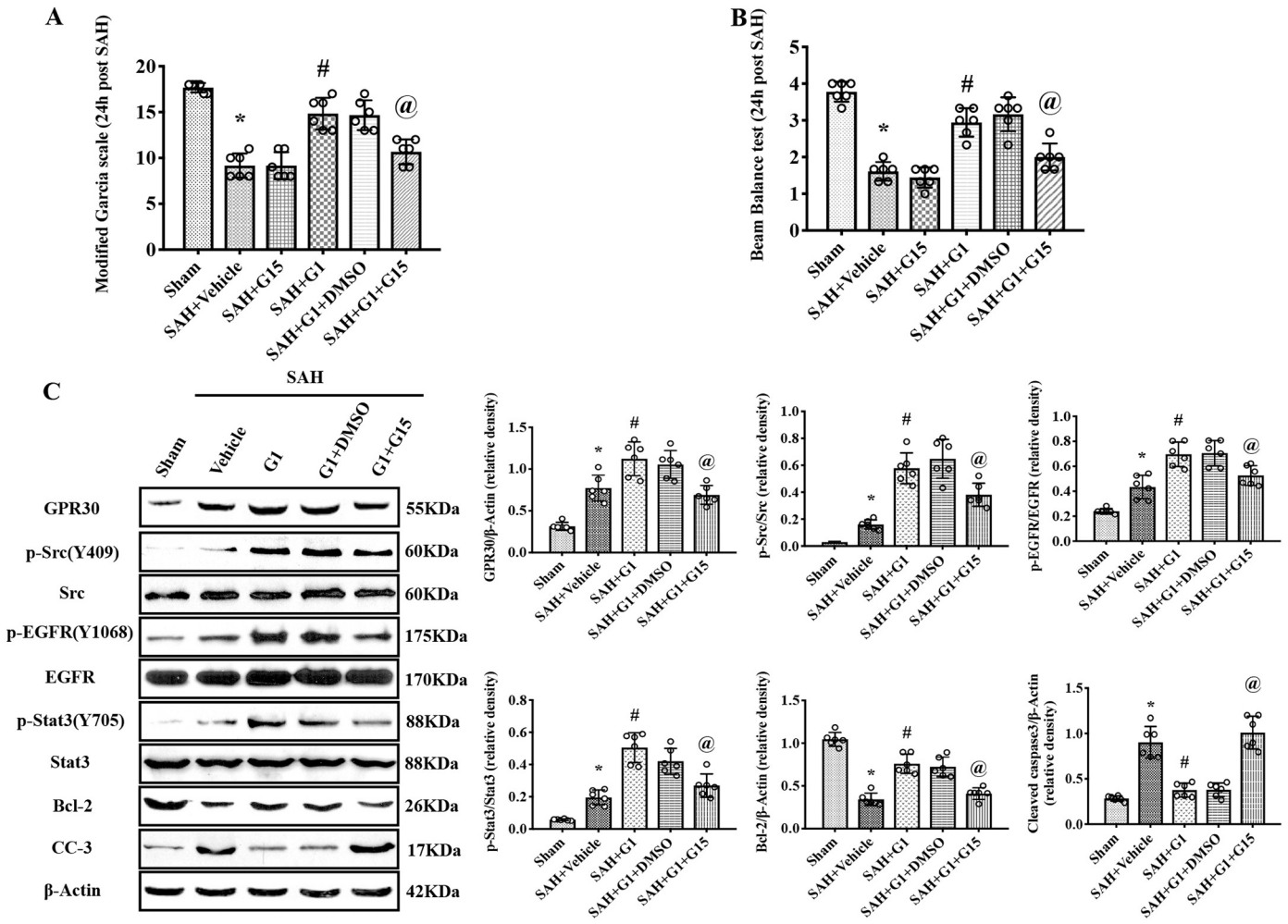

Fig. 7. The G15 reversed the neurological function benefit and anti-neuronal apoptosis effect of G1 in male rats at 24 h after SAH. The performance improvements of Modified Garcia scale (A) and Beam Balance test (B) by G1 treatment in male rats were abolished by G15 at 24 h after SAH. (C) The representative western blot images and quantification analysis of GPR30, p-src/src, p-EGFR/EGFR, p-stat3/stat3, Bcl-2, Cleaved Caspase-3 (CC-3) in the left hemisphere at 24 h after SAH. G1 treatment significantly improved the expressions of GPR30, p-src, p-EGFR, p-stat3 as well as Bcl-2, leading to less level of apoptotic marker CC-3. Such effects were reversed by G15. Data were presented as mean ± SD (n = 6 for each group). $^{*}P < .05$ vs. Sham group, $^{\#}P < .05$ vs. SAH + Vehicle group, $^{@}P < .05$ vs. SAH + G1 + DMSO group.

block 3 (Fig. 5C&D) as well as more time in probe quadrant (Fig. 5F) were observed in SAH + G1 group than SAH + Vehicle group, The swimming velocity among groups was not significant different (Fig. 5E). These results indicated that G1 improved the spatial learning and reference memory functions of male rats at day 25 after SAH.

Nissl staining (Fig. 6) was performed to evaluate the neuronal loss of hippocampus CA1 at day 25 after SAH. The results showed that less surviving neurons in hippocampus CA1 was observed in SAH + Vehicle group compared with sham group, but G1 post-treatment significantly increased the number of surviving neurons in hippocampus CA1 compared with SAH + Vehicle group. It indicated that G1 post-treatment reduced the neuronal loss of hippocampal CA1 at day 25 after SAH in male rats.

3.5. G15 and AG1478 reserved the neuroprotective effect of G1

G15 (Fig. 7A, B) and AG1478 (Fig. 8A, B) were administered to verify the signaling pathway of GPR30 and EGFR underlying the neuroprotective effect of G1 treatment. The results showed that G15 and AG1478 significantly reserved the benefits of G1 treatment on performance of both Modified Garcia scale and Beam Balance test compared with SAH + G1 + DMSO group, either G15 or AG1478 administration alone did not worse the neurological deficits of the rats. The results indicated that GPR30 and EGFR mediated the neuroprotective effect of G1 treatment.

3.6. Activation of GPR30 with G1 attenuated the neuronal apoptosis by preventing down-regulation of Bcl-2 partly via src/EGFR/stat3 signaling pathway

Western blot results (Figs. 7C, 8C, 9) showed that SAH significantly promoted the expression of GPR30, p-src, p-EGFR, p-stat3, Cleaved Caspase-3 and decreased the level of Bcl-2 compared with Sham group. The activation of GPR30 with G1 further up-regulated protein levels of GPR30, p-src, p-EGFR, p-stat3, Bcl-2 but down-regulated Cleaved Caspase-3 expressions significantly compared with SAH + Vehicle group. Pre-treatment with G15 (the GPR30 antagonist) significantly down-regulated the protein level of GPR30, p-src, p-EGFR; p-stat3, Bcl-2 and up-regulated Cleaved Caspase-3 compared with SAH + G1 + DMSO. Pretreatment with AG1478 (the EGFR antagonist) significantly down-regulated the protein level of p-EGFR, p-stat3, Bcl-2 and up-regulated Cleaved Caspase-3 compared with SAH + G1 + DMSO group. Knockdown of GPR30 gene with GPR30 siRNA significantly down-regulated the protein level of GPR30, p-src, p-EGFR; p-stat3, Bcl-2 compared with SAH + G1 + Control siRNA group. Knockdown of EGFR gene with EGFR siRNA significantly down-regulated the protein level of EGFR, p-

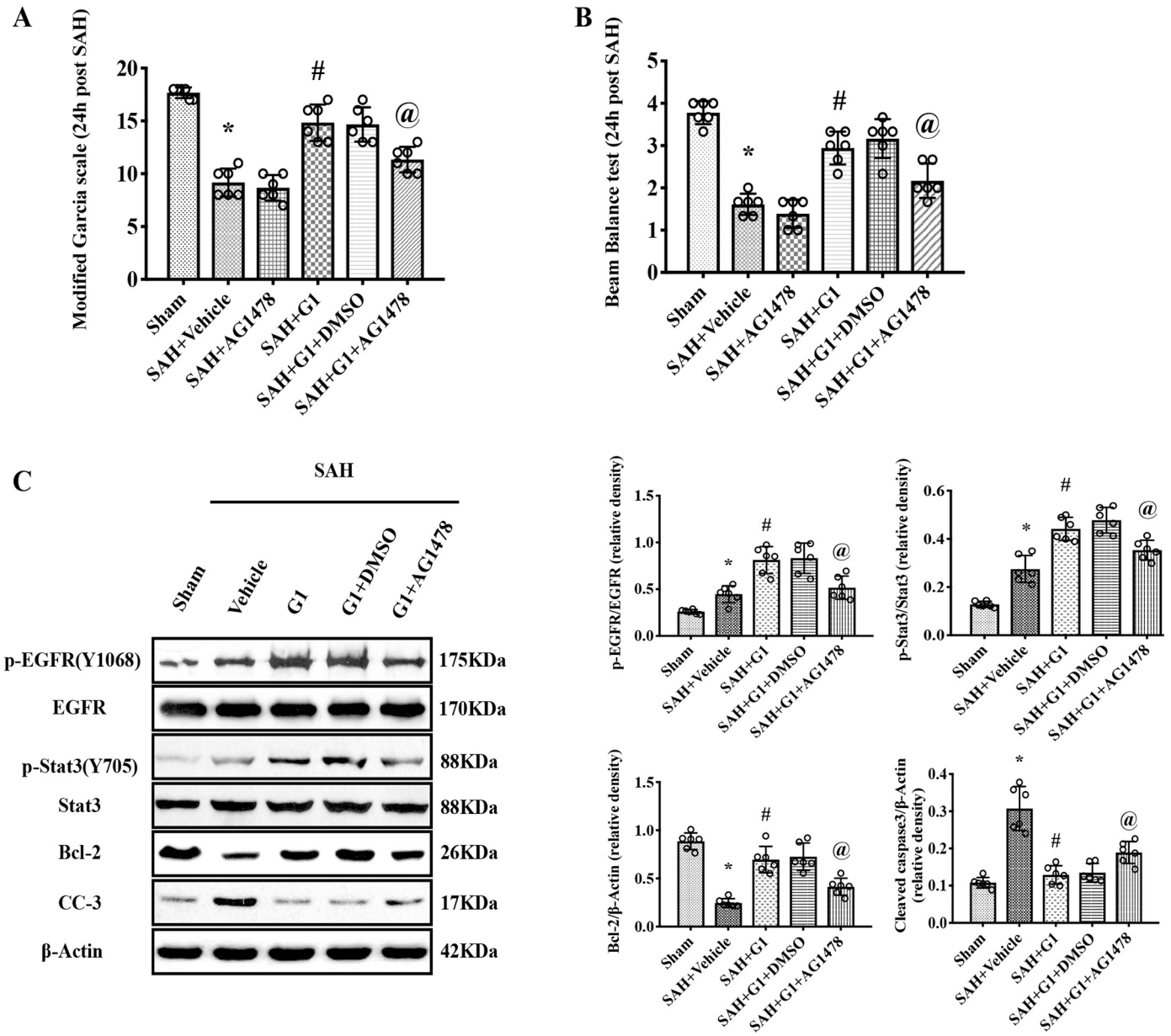

Fig. 8. The AG1478 abolished the neurological function benefit and anti-neuronal apoptosis effect of G1 in male rats at 24 h after SAH. The performance improvements of Modified Garcia scale (A) and Beam Balance test (B) by G1 treatment in male rats were abolished by AG1478 at 24 h after SAH. (C) The representative western blot images and quantification analysis of p-EGFR/EGFR, p-stat3/stat3, Bcl-2, CC-3 in the left hemisphere at 24 h after SAH. AG1478 abolished the G1 induced up-regulation of p-EGFR, p-stat3 and Bcl-2, leading to increased level of apoptotic marker CC-3. Data were presented as mean ± SD (n = 6 for each group), $^{*}P < .05$ vs. Sham group, $^{\#}P < .05$ vs. SAH + Vehicle group, $^{@}P < .05$ vs. SAH + G1 + DMSO group.

EGFR, p-stat3, Bcl-2 compared with SAH + G1 + Control siRNA group. All of these results indicated that activation of GPR30 with G1 attenuated the neuronal apoptosis by preventing down-regulation of Bcl-2 partly via src/EGFR/stat3 signaling pathway at 24 h after SAH.

4. Discussion

In this study, we mainly investigated the effect of GPR30 activation with G1 on neuronal apoptosis and the underlying mechanism in adult male rats after SAH. Our novel findings were: (1) SAH mainly promoted the expression of GPR30 within ipsilateral hemisphere in male rats bot not intact female rats, and GPR30 was mainly expressed by neurons in male rats; (2) G1 post-treatment improved the performance of Modified Garcia scale and Beam Balance test in male rats but not intact female rats, it as well as attenuated neuronal apoptosis at 24 h after SAH in male rats; (3) G1 post-treatment improved the neurobehavioral performance of Rotarod test at week 1 after SAH and Water Maze test at day 25 after SAH, it as well as reduced the neuronal loss of hippocampal CA1 in male rats at day 25 after SAH; (4) G1 post-treatment significantly increased the protein level of GPR30, p-src, p-EGFR, p-stat3 but prevented down-regulation of Bcl-2 in ipsilateral hemisphere at 24 h after SAH in male rats. By antagonizing the GPR30 and EGFR, either G15 or AG1478 significantly reserved the neurobehavioral benefits of G1 and its effects on protein levels of src/EGFR/stat3 signaling pathway involving in anti-apoptosis.

The poor prognosis of SAH had been considered to be related to the delayed cerebral vasospasm for a long time until the EBI was followed with interest by researchers. Numerous studies have shown that EBI also plays crucial role in the prognosis of SAH (Shi et al., 2017; Zhao et al., 2018). In the present study, we reported the contribution of

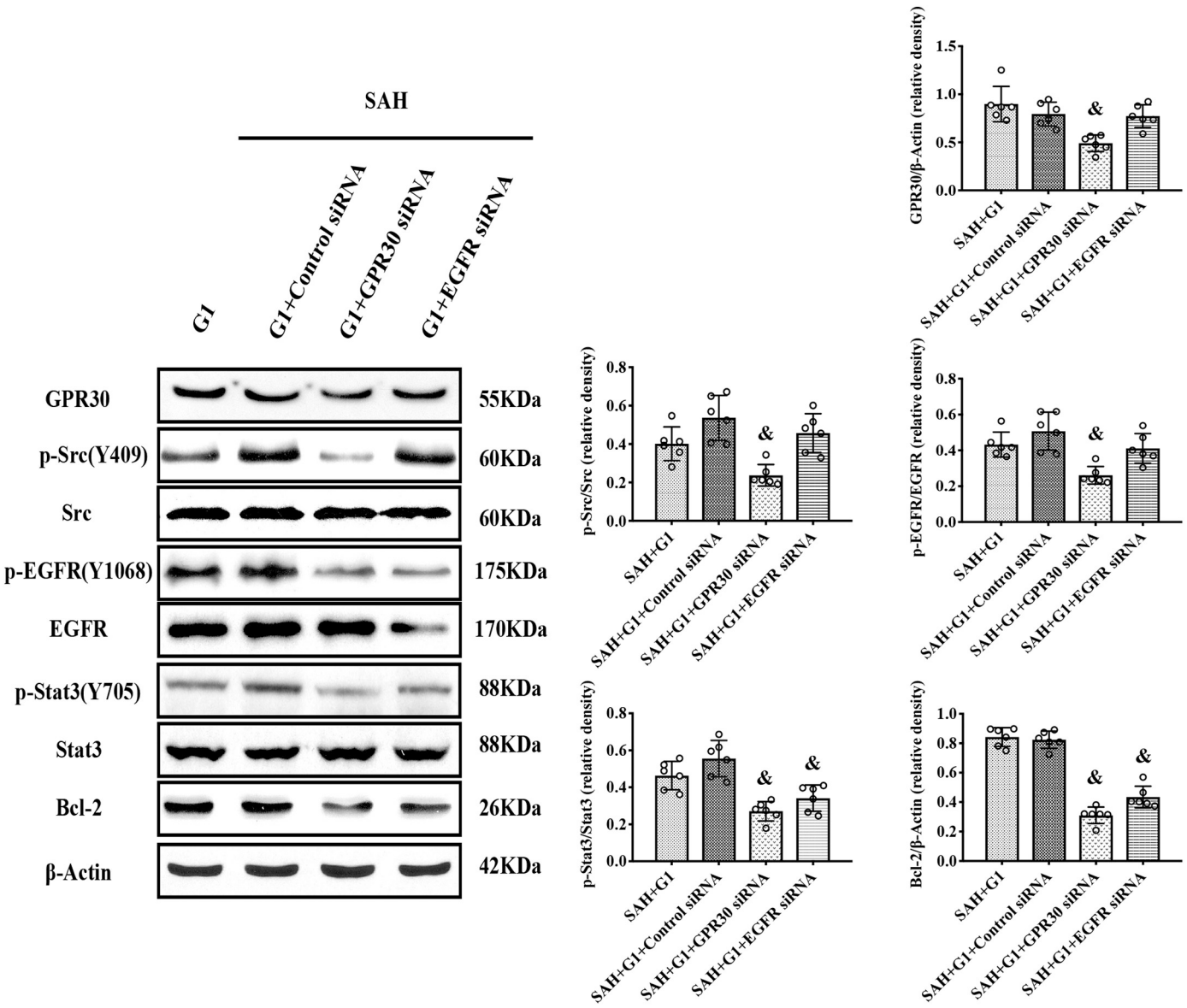

Fig. 9. Gene knockdown of GPR30 or EGFR abolished the neuroprotection effect of G1 at 24 h after SAH. The representative western blot images and quantification analysis of GPR30, p-src/src, p-EGFR/EGFR, p-stat3/stat3, Bcl-2 in the left hemisphere at 24 h after SAH. GPR30 gene knockdown with GPR30 siRNA abolished the G1 induced up-regulation of GPR30, p-src, p-EGFR, p-stat3 and Bcl-2. EGFR gene knockdown with EGFR siRNA abolished G1 induced up-regulation of p-stat3 and Bcl-2. Data were presented as mean ± SD (n = 6 for each group). $^{\&}P < .05$ vs. SAH + G1 + Control siRNA group.

reduced EBI to the improved prognosis of SAH and the role of GPR30 in the process.

GPR30 has been shown to highly expressed in the rat brain regions of anterior and posterior pituitary, granule cells of hippocampus dentate gyrus as well as striatum (Brailoiu et al., 2007; Hazell et al., 2009). It was up-regulated in the hippocampus, somatosensory cortex and hypothalamus only in male but not female mice after focal ischemic stroke and the expression of GPR30 was mainly located in neurons and endothelial cells (Broughton et al., 2013). Consistently, our results showed that SAH promoted the expression of GPR30 in ipsilateral hemisphere in male rats but not female rats. Our double immunofluorescence labeling results also confirmed that GPR30 was highly located in neurons but not astrocytes or microglial cells in male rats. Such endogenous up-regulation of GPR30 may suggest an endogenous neuroprotective mechanism in brain following SAH insult in male rats.

Previous studies demonstrated that the activation of GPR30 with G1 post-treatment at dose of 100 μg/kg and 490 μg/kg (i.v.) exerted anti-apoptotic effect in male rodent model of TBI (Day et al., 2013; Pan et al., 2018). However, it was noted that the time and dose of G1 administration appeared to be critical for its neuroprotective effects in male animals. Pre-treatment with G1 (30μg/kg, i.p) administered 1 h or 2 h prior to ischemia aggravated the outcome of transient focal ischemic stroke in male mice through pro-apoptotic signaling (Broughton et al., 2014). Instead, the pre-treatment with G1 (1.8 mg, subcutaneous pellet over 21 days continuous release) administered at 1 week prior to ischemia enhanced the neuronal survival in male mice subjected to the cardiac arrest induced global brain ischemia (Kosaka et al., 2012). The exact mechanism to determine the pro- or anti-apoptosis fate of G1 in male animals with brain injury needs to be further explored. Nerveless, our results showed that G1 at the dose of 300 μg/kg intravenously delivered at 1 h post-SAH significantly improved the short-term and long-term neurological outcomes of male rats. While the lower dose of 100 μg/kg did not show protective effects, the higher dose of 900 μg/kg did not further improve the neurological performance than that of 300 μg/kg. These neurological benefits were associated with the reduced TUNEL/FJC positive neuron death in male brain tissue after SAH.

But in intact female rats, G1(300 μg/kg)did not show any neuroprotective effect at 24 h after SAH, so we focus our attention on male rats in the mechanism and long-term study.

We further explored the molecular mechanisms underlying the acute neuroprotective effects of G1 mediated by GPR30 in male rats after SAH. Bcl-2 is anti-apoptosis protein participated in the neuroprotective effect of estrogen in both SAH and tMCAO models (Alkayed et al., 2001; Dubal et al., 1999; Kao et al., 2013). In vitro study, G1 protected the cortical neurons from oxidative toxicity and alleviates cell apoptosis by up-regulating Bcl-2 via GPR30 (Liu et al., 2011). In female mice model of spinal cord injury, G1 post-treatment increased the protein levels of GPR30 and Bcl-2 in spinal cord, leading to reduced cell apoptosis and improved motor function (Cheng et al., 2016). In the present study, G1 post-treatment resulted in a higher GPR30 and Bcl-2 protein levels within brain cortex in male rats with SAH, which were associated with less apoptosis markers Cleaved Caspase-3. But in intact female rats, G1 did not increase the expression or the activity of GPR30 to prevent the down-regulation of Bcl-2. The results indicated that G1 post-treatment not only affect the activity but also the expression of GPR30 in male rats, while it had no significant affection on the expression or activity of GPR30 in intact female rats after SAH. We think it should be a compensatory reaction for exogenous stimulations on GPR30, but in intact female rats, because of the high level of endogenous estrogen, the exogenous G1 can hardly affect the activity and expression of GPR30 under the same dose and disease status. Previous studies have suggested activated GPR30 with G1 lead to anti-apoptotic effect by up-regulating Bcl-2 through PI3K/Akt or MAPK/ERK signaling pathway (Cheng et al., 2016; Liu et al., 2011), but the role of stat3 signaling in the anti-apoptotic effect of activated G1 have not been clarified. In experimental ischemic stroke, stat3 phosphorylation has been shown to act as an upstream signaling to promote Bcl-2 transcription underlay the anti-apoptotic effect of estrogen mediated by GPR30 (Dziennis et al., 2007). GPR30 has also been reported to mediate the estrogen-induced stat3 signaling after anorxia (Kwon et al., 2014). Our results showed that SAH increased the expression of p-stat3 in ipsilateral hemisphere at 24 h after SAH, which is consistent with the previous findings in SAH model (Wei et al., 2017). The G1 post-treatment further increased the level of p-stat3 while GPR30 antagonist G15 or knockdown of GPR30 gene with GPR30 siRNA reserved this effect. It suggested that stat3 phosphorylation may participate in the up-regulation of Bcl-2 after activation of GPR30 with G1 in SAH.

In addition, GPR30 was able to transactivate EGFR via src in breast cancer cells (Filardo, 2002; Filardo et al., 2000; Filardo et al., 2002; Luttrell et al., 1999) and oviduct epithelial cells (Popli et al., 2015). After phosphorylation, p-EGFR stimulates up-regulation of downstream ERK1/2 (Filardo et al., 2000) or Akt (Rouhimoghadam et al., 2018) pathway. Thus, we investigated whether the EGFR transactivation mechanism of GPR30 activation contributed to the neuroprotective effects of G1 post-treatment in the present study. The results showed that the expression of p-src and p-EGFR was increased after G1 post-treatment and the effects were reserved after blocking GPR30 with G15 or GPR30 gene knockdown with GPR30 siRNA. Interestingly, previous study has indicated that stat3 can be activated by src directly (Ram and Iyengar, 2001), arguing the participation of EGFR transactivation. In order to confirm the role of EGFR is essential in the anti-apoptotic effect of GPR30 after SAH, a selective EGFR inhibitor AG1478 and EGFR gene knockdown with EGFR siRNA was applied to validate the signaling pathway. We found that protein levels of p-EGFR and p-stat3 were correlated. While G1 treatment significantly increased protein levels of p-EGFR, p-stat3 and Bcl-2, blocking of EGFR with AG1478 and EGFR gene knockdown with EGFR siRNA decreased downstream protein level of p-stat3 and Bcl-2. Our results suggested that the activation of GFPR30 with G1 show neuroprotective effect partly mediated by src/EGFR/stat3 signaling pathway after SAH.

There were some limitations in the present study. Firstly, we only focused our research on neuronal apoptosis. The anti-inflammation (Zhang et al., 2018; Zhao et al., 2016b) and blood brain barrier (BBB) preservation (Lu et al., 2016) of G1 post-treatment need to be further elucidated in SAH model. Secondly, further studies are necessary to confirm the effect of G1 post-treatment under different physiological status and pathological conditions. Thirdly, we demonstrated the important role of src/EGFR/stat3 signaling pathway in the anti-apoptotic effect of G1 post-treatment after SAH. However, we could not exclude the participation of other signaling pathways in the anti-apoptotic effect such as PI3K/Akt or MAPK/ERK1/2 signaling pathway (Cheng et al., 2016; Liu et al., 2011) as well as small-conductance calcium-activated potassium channel 2 (SK2) activation (Kosaka et al., 2012).

5. Conclusion

We concluded that the activation of GPR30 with G1 reduced EBI through attenuating neuronal apoptosis partly via src/EGFR/stat3 signaling pathway at 24 h after SAH in male rats. G1 may provide a promising therapeutic strategy for SAH patients.

Funding sources

This work was supported by the grants from National Institutes of Health (NS081740 and NS082184) to Dr. John, H. Zhang.

Declaration of Competing Interest

We have no conflict of interest to declare.

Acknowledgements

None.

References

Akyol, O., Sherchan, P., Yilmaz, G., Reis, C., Ho, W.M., Wang, Y., Huang, L., Solaroglu, I., Zhang, J.H., 2018. Neurotrophin-3 provides neuroprotection via TrkC receptor dependent pErk5 activation in a rat surgical brain injury model. Exp. Neurol. 307, 82–89.

Alkayed, N.J., Goto, S., Sugo, N., Joh, H.D., Klaus, J., Crain, B.J., Bernard, O., Traystman, R.J., Hurn, P.D., 2001. Estrogen and Bcl-2: gene induction and effect of transgene in experimental stroke. J. Neurosci. 21, 7543–7550.

Brailoiu, E., Dun, S.L., Brailoiu, G.C., Mizuo, K., Sklar, L.A., Oprea, T.I., Prossnitz, E.R., Dun, N.J., 2007. Distribution and characterization of estrogen receptor G protein-coupled receptor 30 in the rat central nervous system. J. Endocrinol. 193, 311–321.

Bromley-Brits, K., Deng, Y., Song, W.H., 2011. Morris water maze test for learning and memory deficits in Alzheimer's disease model mice. J. Vis. Exp. 53, 2920.

Broughton, B.R., Brait, V.H., Guida, E., Lee, S., Arumugam, T.V., Gardiner-Mann, C.V., Miller, A.A., Tang, S.C., Drummond, G.R., Sobey, C.G., 2013. Stroke increases g protein-coupled estrogen receptor expression in the brain of male but not female mice. Neurosignals 21, 229–239.

Broughton, B.R., Brait, V.H., Kim, H.A., Lee, S., Chu, H.X., Gardiner-Mann, C.V., Guida, E., Evans, M.A., Miller, A.A., Arumugam, T.V., Drummond, G.R., Sobey, C.G., 2014. Sex-dependent effects of G protein-coupled estrogen receptor activity on outcome after ischemic stroke. Stroke 45, 835–841.

Burai, R., Ramesh, C., Shorty, M., Curpan, R., Bologa, C., Sklar, L.A., Oprea, T., Prossnitz, E.R., Arterburn, J.B., 2010. Highly efficient synthesis and characterization of the GPR30-selective agonist G-1 and related tetrahydroquinoline analogs. Org. Biomol. Chem. 8, 2252–2259.

Cahill, J., Calvert, J.W., Marcantonio, S., Zhang, J.H., 2007. p53 may play an orchestrating role in apoptotic cell death after experimental subarachnoid hemorrhage. Neurosurgery 60, 531–545.

Cheng, Q., Meng, J., Wang, X.S., Kang, W.B., Tian, Z., Zhang, K., Liu, G., Zhao, J.N., 2016. G-1 exerts neuroprotective effects through G protein-coupled estrogen receptor 1 following spinal cord injury in mice. Biosci. Rep. 36.

Conzen, C., Becker, K., Albanna, W., Weiss, M., Bach, A., Lushina, N., Steimers, A., Pinkernell, S., Clusmann, H., Lindauer, U., Schubert, G.A., 2018. The acute phase of experimental subarachnoid hemorrhage: intracranial pressure dynamics and their effect on cerebral blood flow and autoregulation. Transl. Stroke Res. https://doi.org/10.1007/s12975-018-0674-3.

Day, N.L., Floyd, C.L., D'Alessandro, T.L., Hubbard, W.J., Chaudry, I.H., 2013. 17beta-estradiol confers protection after traumatic brain injury in the rat and involves activation of G protein-coupled estrogen receptor 1. J. Neurotrauma 30, 1531–1541.

Dennis, M.K., Burai, R., Ramesh, C., Petrie, W.K., Alcon, S.N., Nayak, T.K., Bologa, C.G., Leitao, A., Brailoiu, E., Deliu, E., Dun, N.J., Sklar, L.A., Hathaway, H.J., Arterburn, J.B., Oprea, T.I., Prossnitz, E.R., 2009. In vivo effects of a GPR30 antagonist. Nat.

Chem. Biol. 5, 421–427.
Dubal, D.B., Shughrue, P.J., Wilson, M.E., Merchenthaler, I., Wise, P.M., 1999. Estradiol modulates bcl-2 in cerebral ischemia: a potential role for estrogen receptors. J. Neurosci. 19, 6385–6393.
Dziennis, S., Jia, T., Ronnekleiv, O.K., Hurn, P.D., Alkayed, N.J., 2007. Role of signal transducer and activator of transcription-3 in estradiol-mediated neuroprotection. J. Neurosci. 27, 7268–7274.
Filardo, E.J., 2002. Epidermal growth factor receptor (EGFR) transactivation by estrogen via the G-protein-coupled receptor, GPR30: a novel signaling pathway with potential significance for breast cancer. J. Steroid Biochem. Mol. Biol. 80, 231–238.
Filardo, E.J., Quinn, J.A., Bland, K.I., Frackelton Jr., A.R., 2000. Estrogen-induced activation of Erk-1 and Erk-2 requires the G protein-coupled receptor homolog, GPR30, and occurs via trans-activation of the epidermal growth factor receptor through release of HB-EGF. Mol. Endocrinol. 14, 1649–1660.
Filardo, E.J., Quinn, J.A., Frackelton Jr., A.R., Bland, K.I., 2002. Estrogen action via the G protein-coupled receptor, GPR30: stimulation of adenylyl cyclase and cAMP-mediated attenuation of the epidermal growth factor receptor-to-MAPK signaling axis. Mol. Endocrinol. 16, 70–84.
Fujii, M., Yan, J., Rolland, W.B., Soejima, Y., Caner, B., Zhang, J.H., 2013. Early brain injury, an evolving frontier in subarachnoid hemorrhage research. Transl. Stroke Res. 4, 432–446.
Fukada, T., Hibi, M., Yamanaka, Y., Takahashi-Tezuka, M., Fujitani, Y., Yamaguchi, T., Nakajima, K., Hirano, T., 1996. Two signals are necessary for cell proliferation induced by a cytokine receptor gp130: involvement of STAT3 in anti-apoptosis. Immunity 5, 449–460.
Gros, R., Ding, Q., Sklar, L.A., Prossnitz, E.E., Arterburn, J.B., Chorazyczewski, J., Feldman, R.D., 2011. GPR30 expression is required for the mineralocorticoid receptor-independent rapid vascular effects of aldosterone. Hypertension 57, 442–451.
Guo, Z.D., Hu, Q., Xu, L., Guo, Z.N., Ou, Y.B., He, Y., Yin, C., Sun, X.C., Tang, J.P., Zhang, J.H., 2016. Lipoxin A4 reduces inflammation through formyl peptide receptor 2/p38 MAPK signaling pathway in subarachnoid hemorrhage rats. Stroke 47, 490–497.
Hazell, G.G., Yao, S.T., Roper, J.A., Prossnitz, E.R., O'Carroll, A.M., Lolait, S.J., 2009. Localisation of GPR30, a novel G protein-coupled oestrogen receptor, suggests multiple functions in rodent brain and peripheral tissues. J. Endocrinol. 202, 223–236.
Kang, L., Zhang, X., Xie, Y., Tu, Y., Wang, D., Liu, Z., Wang, Z.Y., 2010. Involvement of estrogen receptor variant ER-alpha36, not GPR30, in nongenomic estrogen signaling. Mol. Endocrinol. 24, 709–721.
Kao, C.H., Chang, C.Z., Su, Y.F., Tsai, Y.J., Chang, K.P., Lin, T.K., Hwang, S.L., Lin, C.L., 2013. 17beta-Estradiol attenuates secondary injury through activation of Akt signaling via estrogen receptor alpha in rat brain following subarachnoid hemorrhage. J. Surg. Res. 183, e23–e30.
Kastenberger, I., Lutsch, C., Schwarzer, C., 2012. Activation of the G-protein-coupled receptor GPR30 induces anxiogenic effects in mice, similar to oestradiol. Psychopharmacology 221, 527–535.
Kosaka, Y., Quillinan, N., Bond, C.T., Traystman, R.J., Hurn, P.D., Herson, P.S., 2012. GPER1/GPR30 activation improves neuronal survival following global cerebral ischemia induced by cardiac arrest in mice. Transl. Stroke Res. 3, 500–507.
Kwon, O., Kang, E.S., Kim, I., Shin, S., Kim, M., Kwon, S., Oh, S.R., Ahn, Y.S., Kim, C.H., 2014. GPR30 mediates anorectic estrogen-induced STAT3 signaling in the hypothalamus. Metabolism 63, 1455–1461.
Liu, S.B., Han, J., Zhang, N., Tian, Z., Li, X.B., Zhao, M.G., 2011. Neuroprotective effects of oestrogen against oxidative toxicity through activation of G-protein-coupled receptor 30 receptor. Clin. Exp. Pharmacol. Physiol. 38, 577–585.
Lu, D., Qu, Y., Shi, F., Feng, D., Tao, K., Gao, G., He, S., Zhao, T., 2016. Activation of G protein-coupled estrogen receptor 1 (GPER-1) ameliorates blood-brain barrier permeability after global cerebral ischemia in ovariectomized rats. Biochem. Biophys. Res. Commun. 477, 209–214.
Luttrell, L.M., Daaka, Y., Lefkowitz, R.J., 1999. Regulation of tyrosine kinase cascades by G-protein-coupled receptors. Curr. Opin. Cell Biol. 11, 177–183.
Pan, M.X., Tang, J.C., Liu, R., Feng, Y.G., Wan, Q., 2018. Effects of estrogen receptor GPR30 agonist G1 on neuronal apoptosis and microglia polarization in traumatic brain injury rats. Chin. J. Traumatol. 21, 224–228.
Pang, J., Peng, J., Matei, N., Yang, P., Kuai, L., Wu, Y., Chen, L., Vitek, M.P., Li, F., Sun, X., Zhang, J.H., Jiang, Y., 2018. Apolipoprotein E exerts a whole-brain protective property by promoting M1? Microglia quiescence after experimental subarachnoid hemorrhage in mice. Transl. Stroke Res. 9, 654–668.
Park, O.K., Schaefer, T.S., Nathans, D., 1996. In vitro activation of Stat3 by epidermal growth factor receptor kinase. P. Natl. Acad. Sci. USA 93, 13704–13708.
Popli, P., Sirohi, V.K., Manohar, M., Shukla, V., Kaushal, J.B., Gupta, K., Dwivedi, A., 2015. Regulation of cyclooxygenase-2 expression in rat oviductal epithelial cells: evidence for involvement of GPR30/Src kinase-mediated EGFR signaling. J. Steroid Biochem. Mol. Biol. 154, 130–141.
Ram, P.T., Iyengar, R., 2001. G protein coupled receptor signaling through the Src and Stat3 pathway: role in proliferation and transformation. Oncogene 20, 1601–1606.
Rouhimoghadam, M., Safarian, S., Carroll, J.S., Sheibani, N., Bidkhori, G., 2018. Tamoxifen-induced apoptosis of MCF-7 cells via GPR30/PI3K/MAPKs interactions: verification by ODE modeling and RNA sequencing. Front. Physiol. 9, 907.
Shi, L., Al-Baadani, A., Zhou, K., Shao, A., Xu, S., Chen, S., Zhang, J., 2017. PCMT1 ameliorates neuronal apoptosis by inhibiting the activation of MST1 after subarachnoid hemorrhage in rats. Transl. Stroke Res. https://doi.org/10.1007/s12975-017-0540-8.
Sugawara, T., Ayer, R., Jadhav, V., Zhang, J.H., 2008. A new grading system evaluating bleeding scale in filament perforation subarachnoid hemorrhage rat model. J. Neurosci. Methods 167, 327–334.
Tang, H., Zhang, Q., Yang, L., Dong, Y., Khan, M., Yang, F., Brann, D.W., Wang, R., 2014. Reprint of "GPR30 mediates estrogen rapid signaling and neuroprotection" Mol. Cell. Endocrinol. 389, 92–98.
Thomas, P., Pang, Y., Filardo, E.J., Dong, J., 2005. Identity of an estrogen membrane receptor coupled to a G protein in human breast cancer cells. Endocrinology 146, 624–632.
Wei, S., Luo, C., Yu, S., Gao, J., Liu, C., Wei, Z., Zhang, Z., Wei, L., Yi, B., 2017. Erythropoietin ameliorates early brain injury after subarachnoid haemorrhage by modulating microglia polarization via the EPOR/JAK2-STAT3 pathway. Exp. Cell Res. 361, 342–352.
Xie, Z.Y., Enkhjargal, B., Wu, L.Y., Zhou, K.R., Sun, C.M., Hu, X., Gospodarev, V., Tang, J.P., You, C., Zhang, J.H., 2018. Exendin-4 attenuates neuronal death via GLP-1R/PI3K/Akt pathway in early brain injury after subarachnoid hemorrhage in rats. Neuropharmacology 128, 142–151.
Yan, F., Tan, X., Wan, W., Dixon, B.J., Fan, R., Enkhjargal, B., Li, Q., Zhang, J., Chen, G., Zhang, J.H., 2017. ErbB4 protects against neuronal apoptosis via activation of YAP/PIK3CB signaling pathway in a rat model of subarachnoid hemorrhage. Exp. Neurol. 297, 92–100.
Zhang, Z., Qin, P., Deng, Y., Ma, Z., Guo, H., Guo, H., Hou, Y., Wang, S., Zou, W., Sun, Y., Ma, Y., Hou, W., 2018. The novel estrogenic receptor GPR30 alleviates ischemic injury by inhibiting TLR4-mediated microglial inflammation. J. Neuroinflammation 15, 206.
Zhao, T.-Z., Shi, F., Hu, J., He, S.-M., Ding, Q., Ma, L.-T., 2016a. GPER1 mediates estrogen-induced neuroprotection against oxygen-glucose deprivation in the primary hippocampal neurons. Neuroscience 328, 117–126.
Zhao, T.Z., Ding, Q., Hu, J., He, S.M., Shi, F., Ma, L.T., 2016b. GPER expressed on microglia mediates the anti-inflammatory effect of estradiol in ischemic stroke. Brain Behav. 6, e00449.
Zhao, J., Xiang, X., Zhang, H., Jiang, D., Liang, Y., Qing, W., Liu, L., Zhao, Q., He, Z., 2018. CHOP induces apoptosis by affecting brain iron metabolism in rats with subarachnoid hemorrhage. Exp. Neurol. 302, 22–33.
Zhou, K.R., Enkhjargal, B., Xie, Z.Y., Sun, C.M., Wu, L.Y., Malaguit, J., Chen, S., Tang, J.P., Zhang, J.M., Zhang, J.H., 2018. Dihydrolipoic acid inhibits lysosomal rupture and NLRP3 through lysosome-associated membrane protein-1/calcium/calmodulin-dependent protein kinase II/TAK1 pathways after subarachnoid hemorrhage in rat. Stroke 49, 175–183.